Analysis of Severe Atmospheric Disturbances From Airline Flight Records

R. C. Wingrove, R. E. Bach, Jr., and T. A. Schultz

June 1989

Analysis of Severe Atmospheric Disturbances From Airline Flight Records

R. C. Wingrove, R. E. Bach, Jr., and T. A. Schultz
Ames Research Center, Moffett Field, California

June 1989

ANALYSIS OF SEVERE ATMOSPHERIC DISTURBANCES FROM AIRLINE FLIGHT RECORDS

R. C. Wingrove, R. E. Bach, Jr., and T. A. Schultz
NASA Ames Research Center
Moffett Field, CA 94035

SUMMARY

Advanced methods have been developed to determine time-varying winds and turbulence from digital flight-data recorders carried aboard modern airliners. Analysis of several cases involving severe clear-air turbulence encounters at cruise altitudes has shown that the aircraft encountered vortex arrays generated by destabilized wind-shear layers above mountains or thunderstorms. A model has been developed to identify the strength, size, and spacing of vortex arrays. This model is used to study the effects of severe wind hazards on operational safety for different types of aircraft. The study demonstrates that small remotely piloted vehicles and executive aircraft exhibit more violent behavior than do large airliners during encounters with high-altitude vortices. Analysis of digital flight data from the accident at Dallas/Ft. Worth in 1985 indicates that the aircraft encountered a microburst with rapidly changing winds embedded in a strong outflow near the ground. A multiple-vortex-ring model has been developed to represent the microburst wind pattern. This model can be used in flight simulators to better understand the control problems in severe microburst encounters.

1. INTRODUCTION

Flight encounters with severe atmospheric disturbances are a continuing problem that must be better understood to improve safety. One way to investigate the nature and cause of severe disturbances is through the analysis of airline flight records. In the past, analysis was hindered by insufficient data. Recent encounters have involved modern airliners equipped with multichannel, digital flight-data recorders (DFDRs). These digital records, along with air traffic control (ATC) radar position records, provide a means of determining and analyzing the turbulent wind environment (Ref. 1).

In conjunction with the National Transportation Safety Board (NTSB), researchers from Ames Research Center have analyzed a series of disturbance encounters, listed in Table I, involving airliners equipped with DFDRs. The severe atmospheric disturbances to be considered in this report include high-altitude turbulence and low-level microbursts.
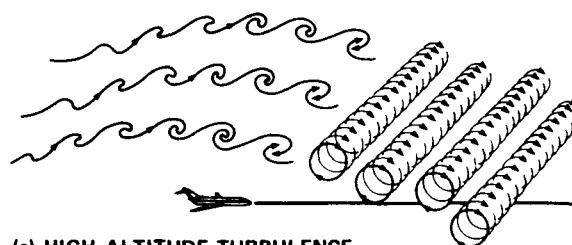
TABLE I – DIGITAL FLIGHT RECORDS FROM AIRLINE ENCOUNTERS WITH SEVERE ATMOSPHERIC DISTURBANCES.

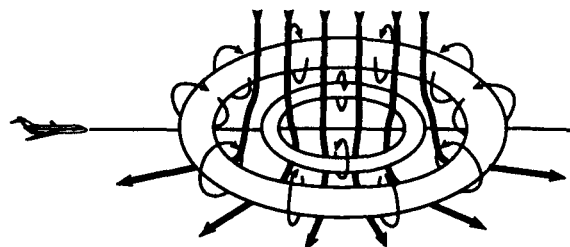| DATE	AIRCRAFT	LOCATION	OPERATION	DISTURBANCE
6/75	L1011	JFK, NY	Go-around	Microburst
11/75	DC10	Calgary, Canada	33,000'	Clear air turbulence
4/81	DC10	Hannibal, MO	37,000'	Clear air turbulence
7/82	DC10	Morton, WY	39,000'	Clear air turbulence
10/83	DC10	Near Bermuda	37,000'	Convective turbulence
11/83	L1011	Offshore SC	37,000'	Clear air turbulence
1/85	B747	Over Greenland	33.000'	Clear air turbulence
2/85	B747	Over Greenland	33,000'	Clear air turbulence
2/85	B747SP	Offshore CA	41,000'	Wind shear
8/85	L1011	Dallas/Ft.Worth, TX	Landing	Microburst
8/85	MD80	Dallas/Ft.Worth, TX	Go-around	Microburst
11/85	B747	Over Greenland	33,000'	Clear air turbulence
3/86	B747	Offshore Hawaii	33,000'	Clear air turbulence
4/86	DC10	Jamestown, NY	40,000'	Wind shear
7/86	A300	West Palm Beach, FL	20,000'	Convective turbulence
9/87	L1011	Near Bermuda	31,000'	Convective turbulence
11/87	A310	Near Bermuda	33,000'	Convective turbulence
1/88	B767	Chicago, IL	25,000'	Convective turbulence
3/88	B767	Cimarron, NM	33,000'	Clear air turbulence

High-altitude turbulence (Fig. 1a) results from the growth and breakdown of stratified shear layers (Refs. 2-7). This disturbance is usually referred to as "clear-air turbulence" and is associated with a strong inversion in air temperature and a strong vertical shear in horizontal winds. These conditions are often in the regions of the tropopause and the associated jet streams. The most severe encounters are frequently above mountains or thunderstorms. Some of the severe clear-air turbulence encounters for airliners equipped with the DFDR are discussed in Refs. 8-10.

Microbursts (Fig. 1b) are intense downdrafts that impact the surface and cause strong outflows (Refs. 11-13). They are associated with thunderstorms, and usually occur during the summer. The accident of Delta Airlines flight 191 in August 1985 involved a microburst at the Dallas/Ft.Worth airport (DFW). This aircraft and the following American Airlines flight 539, which made a go-around through the DFW microburst, were both equipped with DFDRs. Some background information about the DFW microburst can be found in Refs. 14-20.

(a) HIGH-ALTITUDE TURBULENCE

This paper considers the usefulness of DFDR data in analyzing aircraft encounters with clear-air turbulence and low-level microbursts, and presents some findings regarding the nature of these phenomena. In particular, it is shown that the winds encountered in both types of atmospheric disturbances can be modeled deterministically. In the case of clear-air turbulence, the winds are represented by a Kelvin-Helmholtz vortex-array model. In the case of the DFW microburst, the winds are represented by a multiple-vortex-ring model. The method used to analyze the the flight records is described first. Its application to clear-air turbulence encounters is presented, followed by an analysis of the DFW microburst encounter.

(b) LOW-LEVEL MICROBURST

Figure 1. Two types of severe atmospheric disturbances.

2. ANALYSIS METHOD

Airliners certified in 1969 or later are equipped with DFDRs which record an extensive set of variables (Table II). These digital flight records, along with ATC tracking data, can be used to determine the time histories in the three components of the winds along the aircraft flightpath (Ref. 1). In this analysis the accelerations measured aboard the aircraft are integrated to determine the time history of the flightpath that provides the best match to the ATC radar position data and the DFDR barometric altitude data. The wind velocity is computed as the difference between the vehicle inertial velocity and its velocity with respect to the airmass. A block diagram of the general analysis procedure is shown in Fig. 2.

The equations of motion are in an Earth frame with the x-axis pointing north, the y-axis pointing east, and the h-axis vertical (z axis down):

$$\ddot{x} = a_x \cos\theta \cos\psi + a_y(\sin\phi \sin\theta \cos\psi - \cos\phi \sin\psi) + a_z(\cos\phi \sin\theta \cos\psi + \sin\phi \sin\psi)$$

$$\ddot{y} = a_x \cos\theta \sin\psi + a_y(\sin\phi \sin\theta \sin\psi + \cos\phi \cos\psi) + a_z(\cos\phi \sin\theta \sin\psi - \sin\phi \cos\psi)$$

$$\ddot{h} = a_x \sin\theta - (a_y\sin\phi + a_z\cos\phi)\cos\theta - g$$

where a_x, a_y, and a_z are the body-axis accelerations, and ϕ, θ, and ψ are the body-axis Euler angles. Integration of these differential equations provides estimates of inertial velocity $(\dot{x},\dot{y},\dot{h})$ and position (x,y,h). A set of initial conditions and bias corrections is determined by matching the calculated x and y time-histories to ATC radar position data and by matching the calculated h time history to the DFDR barometric altitude data.

TABLE II – TYPICAL DIGITAL FLIGHT DATA RECORDER MEASUREMENTS FOR DIFFERENT AIRCRAFT.

VARIABLE	MEASUREMENT RATE, per sec					
	L1011	DC10	MD80	B747	B747SP	B767
Normal acceleration	4	4	8	4	4	4
Lateral acceleration	4	4	4	4	4	4
Longitudinal acceleration	4	1	4	4	4	1
Roll angle	1	1	1	1	1	1
Pitch angle	1	1	1	1	1	1
Heading angle	1	1	1	1	1	1
Angle-of-attack vanes	2	-	-	-	2	2
Pressure altitude	1	1	1	1	1	1
Indicated airspeed	1	1	1	1	1	1
Elevator deflection	1	1	1	1	1	1
Rudder deflection	2	2	2	2	2	2
Engine thrust	1/4	1/4	1	1/4	1/4	1
Air temperature	1/2	1/2	1	-	-	1

The wind vector is computed as

$$W_x = \dot{x} - V \cos\psi_a \cos\gamma_a$$

$$W_y = \dot{y} - V \sin\psi_a \cos\gamma_a$$

$$W_h = \dot{h} - V \sin\gamma_a$$

where the true airspeed V is computed from the flight records, and the wind-axis Euler angles (γ_a, ψ_a) are computed using the identities

$$\sin\gamma_a = \cos\alpha \cos\beta \sin\theta - C \cos\theta$$

$$\tan(\psi_a - \psi) = (\sin\beta \cos\phi - \sin\alpha \cos\beta \sin\phi)/(\cos\alpha \cos\beta \cos\theta + C \sin\theta)$$

$$C = \sin\alpha \cos\beta \cos\phi + \sin\beta \sin\phi$$

where α is the angle of attack and β is the angle of sideslip.

The angle of attack α was derived from onboard-recorded vane angles. For aircraft without recorded vane angles, the angle of attack α was determined through the equation

$$C_L = C_L(\alpha, \delta_f) + C_{L\delta e}\, \delta_e + C_{Lq}(\bar{c}q/2V)$$

Figure 2. Reconstruction of severe winds from flight and ATC records.

where $C_L(\alpha, \delta_f)$, $C_{L\delta e}$, and C_{Lq} are based on the aircraft aerodynamic characteristics, and the lift coefficient C_L was calculated using the aircraft weight along with the lift acceleration and dynamic pressure from the DFDR. The flap position δ_f, elevator position δ_e, and pitch rate q were derived from the DFDR, leaving the angle of attack α as the variable to be determined. (This method of deriving unmeasured flow angles is discussed further in Ref. 21.)

In a similar manner, the angle of sideslip β was determined through the equation

$$C_Y = C_{Y\beta}\beta + C_{Y\delta r}\delta_r + C_{Yr}(br/2V)$$

where $C_{Y\beta}$, $C_{Y\delta r}$, and C_{Yr} are based on the aircraft aerodynamic characteristics, and the side-force coefficient C_Y was calculated using the aircraft weight along with the side acceleration and dynamic pressure from the DFDR. The rudder position δ_r and the yaw rate r were derived from the DFDR, leaving the angle of sideslip β as the variable to be determined.

3. APPLICATIONS

3.1 High-Altitude Turbulence

High-altitude clear-air turbulence encounters usually occur in the region of the tropopause. The tropopause altitude varies with the season and the location. The upper plot in Fig. 3 shows recent severe turbulence encounters as a function of altitude and time of year. Also shown are the average tropopause heights for 30° and 45° N. lat. (Ref. 22). Generally, this distribution of turbulence encounters follows the trends for the average tropopause heights. That is, the encounters occur at lower altitudes in the winter months and at higher altitudes in the summer months. The lower plot in Fig. 3 presents the distribution of 12,678 reports of moderate to severe turbulence, from a special survey of airline pilots taken in 1960-62 (Ref. 7). These data indicate that turbulence occurred most often in the winter months, peaking in February. At the time of the survey, airliners usually cruised at altitudes of 31,000 to 33,000 ft, and would be in the region of the tropopause primarily in the winter months. However, many of today's aircraft cruise at higher altitudes, and spend more time in the region of the tropopause throughout the year. At altitudes from 35,000 to 41,000 ft the aircraft are in the region of the tropopause in the fall and spring.
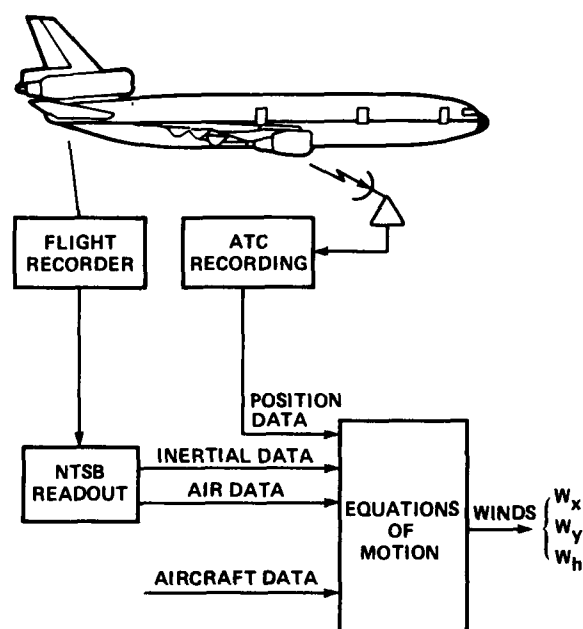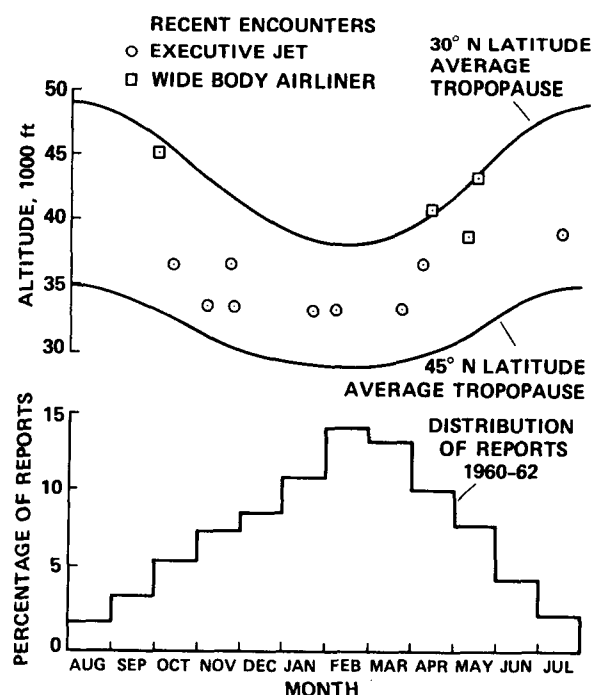

Figure 3. Severe turbulence encounters shown with altitude and time of year.

Many clear-air-turbulence encounters occurred near or over a landmass where meteorological soundings provide wind and temperature profiles, ground weather radar observations provide information about nearby convective activity, and ATC radar records provide information about the aircraft track. Representative encounters are illustrated in Fig. 4. Note that the encounters were associated with low-level barriers such as mountain ranges or thunderstorm lines. The encounters were found to occur at about 15 to 30 miles downwind of these low-level obstacles.

Temperature profiles for the encounters of Fig. 4 are presented in Fig. 5. The sounding records in Fig. 5 indicate a strong temperature inversion at the tropopause. Previous studies (Refs. 2-4) have noted that a strong temperature inversion becomes a destabilizing influence when the streamlines are tilted. The encounters analyzed here involved temperature inversions in conjunction with lower-level barriers that could have tilted the streamlines and triggered Kelvin-Helmholtz instability (Refs. 2-4).
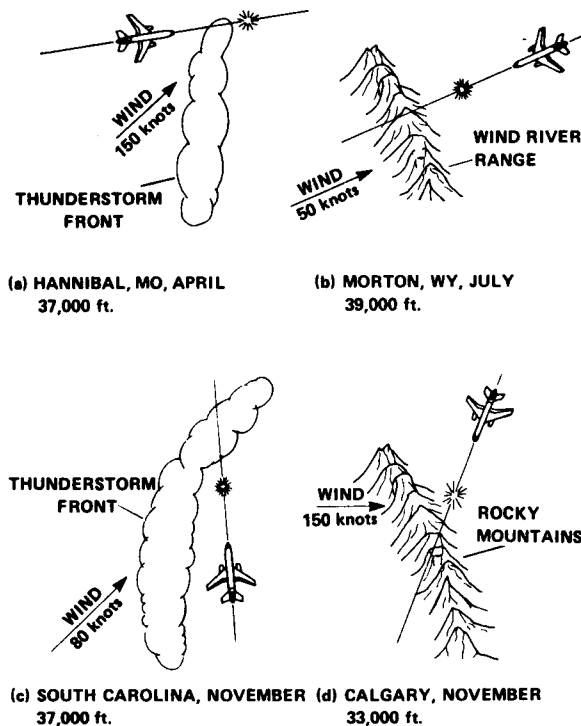
WIND 150 knots

THUNDERSTORM FRONT

(a) HANNIBAL, MO, APRIL 37,000 ft.

WIND 50 knots

WIND RIVER RANGE

(b) MORTON, WY, JULY 39,000 ft.

THUNDERSTORM FRONT

WIND 80 knots

WIND 150 knots

ROCKY MOUNTAINS

(c) SOUTH CAROLINA, NOVEMBER 37,000 ft.

(d) CALGARY, NOVEMBER 33,000 ft.

Figure 4. Overview of severe turbulence encounters at cruise altitudes.

ALTITUDE, 1000 ft

(a) HANNIBAL, MO, APRIL

(b) MORTON, WY, JULY

(c) SOUTH CAROLINA, NOVEMBER

(d) CALGARY, NOVEMBER

-70   -50   -30
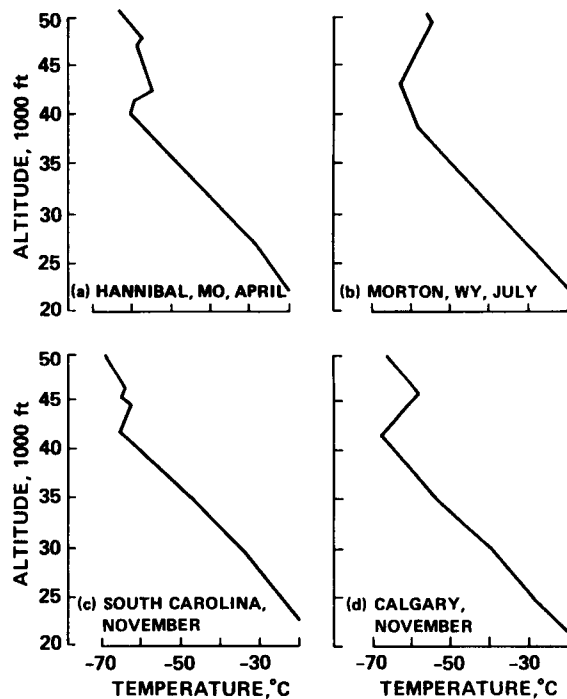TEMPERATURE, °C

-70   -50   -30
TEMPERATURE, °C

Figure 5. Temperature inversion at the tropopause associated with severe turbulence.

A representative case is that of Fig. 4a, in which a DC-10 encountered severe turbulence while cruising in an easterly direction at 37,000 ft in the jet steam in April near Hannibal, Missouri (Ref. 8). The encounter occurred shortly after the aircraft passed over a developing line of thunderstorms with cloud tops reported at about 30,000 ft. Using the technique described in the previous section, the horizontal wind W_x and vertical wind W_h were estimated. These estimates and the normal acceleration from the DFDR are presented in Fig. 6. The horizontal wind is shown to increase as the aircraft passes over the line of thunderstorms about 2.5 min before the turbulence encounter. The vertical winds in the period of severe turbulence appear as sharp up-and-down gusts about 5 sec apart. The severity of the turbulence is apparent from the wide fluctuations in the normal acceleration from +1.7 to –1.0 g.

These results appear consistent with previous studies (Refs. 2-6) in which the formation of Kelvin "cat's eyes" patterns in clear air was noted. To determine whether the derived winds could be accounted for by patterns of this type, an analysis was conducted to duplicate the time histories with vortex-array models (Refs. 8, 23). The DFDR-derived wind data were used with parameter identification techniques to determine the strength, size, and spacing of the vortex arrays. A vortex model for the Hannibal case is shown in Fig. 7. As shown in the lower graph, the general nature of this model is a vortex array located on the downslope with respect to the prevailing wind. The large spikes in vertical velocity are caused by the passage of the aircraft through the solid-body cores of two vortices. These spikes provide significant evidence about the size and strength of the vortices. Each vortex has a diameter of 1,000 ft and a circumferential velocity of 87 ft/sec. The distance between the centers of the two significant vortices is 3,400 ft. A comparison of the modeled vertical and horizontal wind perturbations (solid lines) with the measured winds (dashed lines) shows reasonably good agreement. This vortex model provides a means of studying the effects of these wind hazards on aircraft behavior and g load.

Simulations have been done to provide information on the effects of these reconstructed vortices on the flight behavior for three types of aircraft: a remotely piloted vehicle (RPV), an executive jet, and a large commercial airliner. As shown in Fig. 8, the RPV undergoes a large change in pitch angle. With its relatively low speed, it has time to align with the local airspeed vector, and the pattern of the pitch angle variation is similar to the (inverse) pattern of the vertical wind. The executive aircraft exhibits periodic variations in pitch angle and g load. These variations are dependent upon the relationship between the time span of the vortex traverse and the aircraft's short oscillatory period. The large airliner exhibits only a small variation in pitch angle, because of the short time in vortex traverse and a long oscillatory period. The pattern of the g-load variation is similar to the pattern of the vertical wind.
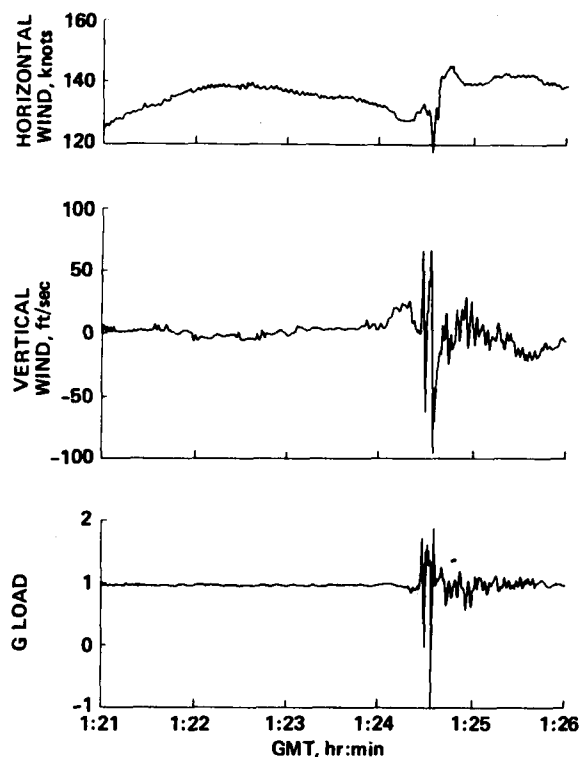
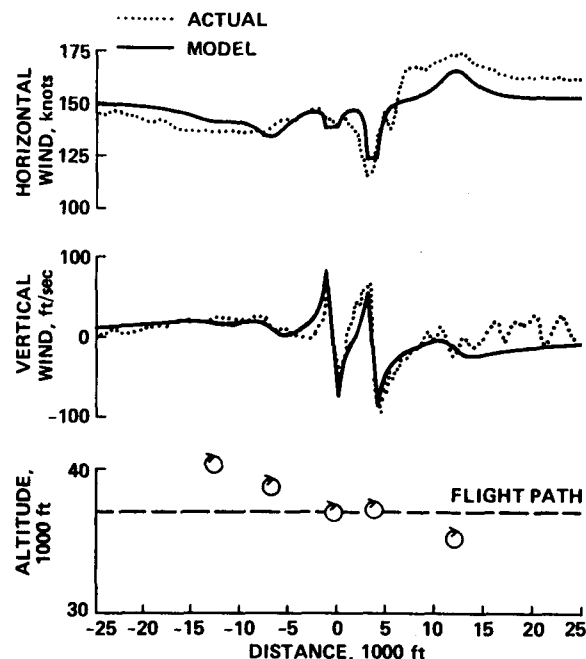Figure 6. Time-history data for a severe turbulence encounter over Hannibal, MO, April 1981.

Figure 7. Vortex-array model for a severe turbulence encounter over Hannibal, MO, April 1981.

3.2 Low-Level Microbursts

Flight and radar records from two airliners that penetrated the 1985 DFW microburst have been analyzed. The first aircraft, Delta Airlines flight 191, encountered the microburst on final approach and contacted the ground about 1 mile short of the runway. The following aircraft, American Airlines flight 539, made a go-around and flew through the microburst about 2,500 ft above the ground. The results of the analysis are shown in Fig. 9. The data for the two aircraft are presented as a function of altitude and position with respect to the runway. The horizontal and vertical wind components (W_x and W_h) are superimposed as vectors on the flightpaths.

As Delta 191 descended through 900 ft approaching the runway, the vertical wind component W_h increased to about 15 ft/sec and the horizontal wind component W_x increased to a headwind of over 50 ft/sec. The aircraft then encountered a strong downflow followed by a rapid change in vertical wind direction, followed by further changes about 5 sec apart. In the period of major downflow, the aircraft experienced vertical winds of –10 to –40 ft/sec. During the encounter, the 50-ft/sec headwind changed to a tailwind of over 50 ft/sec.

American 539, the following aircraft, executed a go-around at 1400 ft above the ground and then climbed to an altitude of 2500 ft where it penetrated the microburst. The analysis shows that the aircraft first experienced an updraft W_h of about 15 ft/sec and a headwind W_x of 15 ft/sec. The aircraft then encountered a strong downflow over a fairly large distance, followed by a strong updraft. In the period of major downflow, the aircraft experienced vertical winds of –10 to –40 ft/sec. During this encounter, the 15 ft/sec headwind changed to a tailwind of over 25 ft/sec.
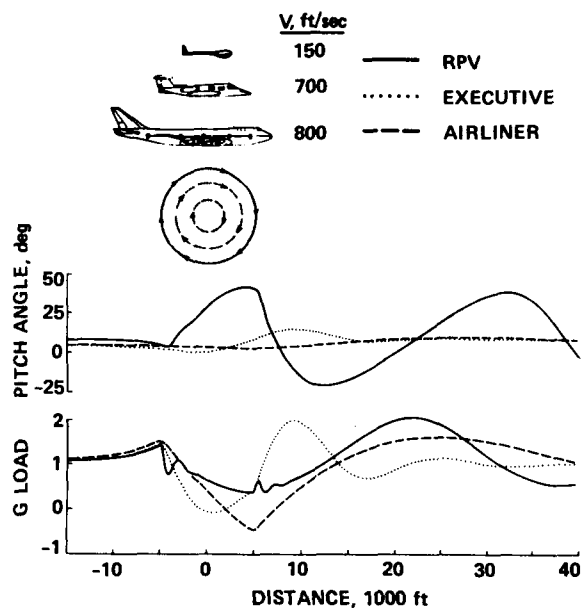

Figure 8. Simulation of a vortex encounter for different aircraft.

In comparing the magnitudes of the changes in the horizontal winds W_x, we can see that Delta 191 was nearer the ground and experienced the stronger horizontal divergence from the microburst. The data indicate that there was a head-wind-tailwind change of 100 ft/sec for Delta 191, and 40 ft/sec for American 539. Note that the overall change from a head-wind to a tailwind occurred at nearly the same location over the ground for the two aircraft. This suggests that the center of the microburst had not changed location appreciably between the times that the two sets of measurements were made. American 539 passed through the center of the microburst about 110 sec after Delta 191 did.

It can be observed that the region of the downflow measured for American 539 is larger than that for Delta 191. American 539 entered the region of the downflow about 0.5 n. mi. farther out from the runway than did Delta 191. Also, the data from American 539 indicate that portions of the downflow had extended to near the end of the runway. The total region of downflow measured by American 539 was about 3 n. mi. in diameter. This indication of an expanding microburst is consistent with meteorological data gathered at the DFW airport (Ref. 16) and with a numerical simulation of the DFW downburst (Ref. 19). These studies indicate that the storm had reached the end of the runway and had expanded to about 3.7 n. mi. in diameter near ground level when American 539 traversed the microburst.

The Ames analysis shows several rapid and large changes in winds within the microburst. Previous studies (Refs. 12, 24-26) have indicated that microbursts might involve vortices that induce variations in the internal winds. Those studies indicate that when a vortex nears the ground its vorticity increases, providing a mechanism for large fluctuations in wind velocity.

A multiple-vortex-ring model has been developed to represent the wind pattern in the DFW microburst (Ref. 27). The vortex model for American 539, which made a complete passage through the microburst, is shown in Fig. 10. As shown in the lower graph, the general nature of this model is a large outer ring with a smaller inner ring near the center of the microburst. The outer ring has a diameter of 15,000 ft with a vortex core diameter of 3000 ft. The inner ring has a diameter of 2500 ft with a vortex core diameter of 900 ft. A comparison of the modeled vertical and horizontal wind perturbations (solid lines) with the measured winds (dashed lines) shows reasonably good agreement. The multiple-vortex-ring model provides a way to mathematically describe the wind pattern within the microburst. The model provides a deterministic, rather than random, means of analyzing the internal velocity fluctuations.

Figure 9. Wind vectors at the Dallas/Ft.Worth Airport, August 1985, reconstructed from flight records of two aircraft.

Figure 10. Multiple-vortex-ring model of the DFW microburst.

4. CONCLUDING REMARKS

Analysis of a series of cases involving severe turbulence at cruise altitudes has shown that the aircraft encountered vortex arrays generated by wind-shear layers associated with strong temperature inversions near the tropopause. The destabilization of the wind-shear layers was caused by low-level barriers such as mountain ranges or thunderstorm lines. The wind pattern in these severe turbulence encounters have been identified through the development of vortex-array models. The analysis identified the strength, size, and spacing of the vortex arrays, providing a means of studying the effects of these severe wind hazards on operational safety. Modern aircraft are spending more time at higher altitudes near the tropopause, where this severe turbulence occurs. Simulation studies have shown that small RPV and executive aircraft are more prone to violent dynamic behavior than are large airliners during encounters with high-altitude vortices .

Data from the Delta 191 accident show that the aircraft encountered a strong microburst downflow followed by a strong outflow accompanied by large and rapid changes in vertical wind. Data from American 539 recorded during the go-around indicate a broad pattern of downflow in the microburst, with regions of upflow at the extreme edges. The combined results indicate a microburst that was increasing in size with vortex-induced velocity fluctuations embedded in a strong outflow near the ground. The wind pattern in the DFW microburst has been identified through the development of a multiple-vortex-ring model. The results show a large vortex ring at the leading edge of the microburst and a smaller vortex ring embedded in the downflow. The study provides a realistic model of the wind field that can be used in flight simulators to better understand the control problems in severe microburst encounters.
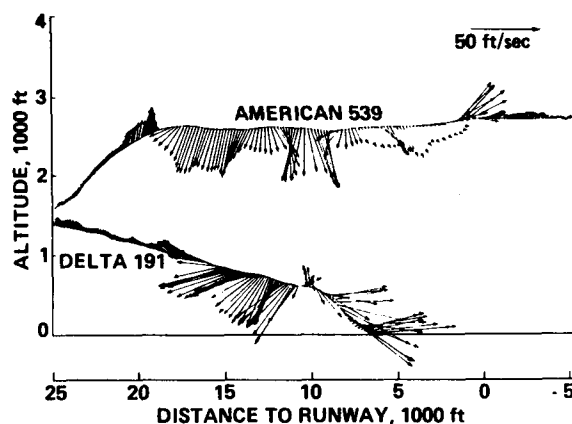
5. REFERENCES

1. Bach, R. E. and Wingrove, R. C., "Applications of State Estimation in Aircraft Flight-Data Analysis." J. Aircraft, Vol. 22, No. 7, July 1985, pp. 547-554.

2. Scorer, R. S., "Environmental Aerodynamics." Wiley, New York, 1978.

3. Gossard, E. E. and Hooke W. H., "Waves in the Atmosphere." Elsevier Scientific Publishing Co., New York, 1975.

4. Clark, J. W., Stoeffler, R. C., and Vogt, P. G., "Research on Instabilities in Atmospheric Flow Systems Associated with Clear Air Turbulence." NASA CR-1604, 1970.

5. Hopkins, R. H., "Forecasting Techniques of Clear Air Turbulence Including That Associated with Mountain Waves." WMO Technical Note No. 155, 1976.

6. Hardy, K. R., "Studies of the Clear Atmosphere Using High Power Radar." Remote Sensing of the Troposphere, V. E. Derr, ed., NOAA, Boulder CO, 1972, chap. 14.

7. Colson, DeVer, "Summary of High-Level Turbulence Over United States." Monthly Weather Review, Vol. 91, No. 12, 1963, pp. 605-609.

8. Parks, E. K., Wingrove, R. C., Bach, R. E., and Mehta, R. S., "Identification of Vortex-Induced Clear Air Turbulence Using Airline Flight Records." J. Aircraft, Vol. 22, No. 2, Feb. 1985, pp. 124-129.

9. Lester, P.F. and Bach, R. E., "An Extreme Clear Air Turbulence Incident Associated with a Strong Downslope Windstorm." AIAA Paper 86-0329, Jan. 1986.

10. Lester, P., Sen, O., and Bach, R. E., "The Use of DFDR Information in the Analysis of a Turbulence Incident Over Greenland." Monthly Weather Review, accepted for publication June 1989.

11. "Low-Altitude Wind Shear and Its Hazard to Aviation." National Academy of Sciences, National Academy Press, Washington, D.C., 1983.

12. Fujita, T. T., "The Downburst." SMRP Research Paper 210, U. Chicago, Chicago Ill., 1985.

13. "Windshear Training Aid." Federal Aviation Administration, Washington, D.C. 1987.

14. Bach, R. E. and Wingrove, R. C., "Analysis of Windshear from Airline Flight Data." J. Aircraft, Vol. 26, No. 2, Feb. 1989, pp. 103-109.

15. Wingrove, R. C. and Bach, R. E., "Severe Winds in the DFW Microburst Measured from Two Aircraft." J. Aircraft, Vol. 26, No. 3, March 1989, pp. 221-224.

16. Fujita, T. T., "DFW Microburst." SMRP Research Paper 217, U. Chicago, Chicago Ill., 1985.

17. Caracena, F., Ortiz, R., and Augustine, J., "The Crash of Delta Flight 191 at Dallas-Fort Worth International Airport on 2 August 1985: Multiscale Analysis of Weather Conditions." NOAA Technical Report ERL 430-ESG 2, Dec. 1986.

18. Aircraft Accident Report, "Delta Air Lines Inc., Lockheed L-1011-385-1, N726DA, Dallas/Fort Worth International Airport, Texas, August 2, 1985." NTSB AAR-86-05, 1986.

19. Proctor, F. H., "The Terminal Area Simulation System, Volume II, Verification Cases." NASA CR 4047, April 1987.

20. Bray, R. S., "Aircraft Performance in Downburst Wind Shear." SAE Paper No. 861698, 1986.

21. Bach, R. E. and Parks, E. K., "Angle-of-Attack Estimation for Analysis of CAT Encounters." J. Aircraft, Vol. 24, No. 11, Nov. 1987, pp. 789-792.

22. Roe, J. M., "A Climatology of a Newly-Defined Tropopause Using Simultaneous Ozone-Temperature Profiles." AFGL-TR-81-0190, May 1981.

23. Mehta, R. S., "Modeling Clear-Air Turbulence with Vortices Using Parameter-Identification Techniques." J. Guidance, Contr. Dynam., Vol. 10, No. 1, Jan. 1987, pp. 27-31.

24. Caracena, F., "Is the Microburst a Large Vortex Ring Imbedded in a Thunderstorm Downdraft?" Eos, Vol. 63, 1982, p. 899.

25. Woodfield, A. A. and Woods, J. F., "Worldwide Experience of Wind Shear During 1981-1982." AGARD-CP-347, Oct. 1983.

26. Bedard, A., "Microburst Vorticity." AIAA Paper 87-0440, 1987.

27. Schultz, T. A., "A Multiple-Ring-Vortex Model of the DFW Microburst." AIAA Paper 88-0685, Jan. 1988.

ACKNOWLEDGMENT

NASA
National Aeronautics and Space Administration

Report Documentation Page

1. Report No. NASA TM-102186	2. Government Accession No.	3. Recipient's Catalog No.
4. Title and Subtitle Analysis of Severe Atmospheric Disturbances From Airline Flight Records		5. Report Date June 1989
		6. Performing Organization Code
7. Author(s) R. C. Wingrove, R. E. Bach, Jr., and T. A. Schultz		8. Performing Organization Report No. A-89111
		10. Work Unit No. 505-66-41
9. Performing Organization Name and Address Ames Research Center Moffett Field, CA 94035		11. Contract or Grant No.
		13. Type of Report and Period Covered Technical Memorandum
12. Sponsoring Agency Name and Address National Aeronautics and Space Administration Washington, DC 20546-0001		14. Sponsoring Agency Code

15. Supplementary Notes

This document was originally prepared for the AGARD Flight Mechanics Panel Symposium—Flight in Adverse Environmental Conditions, Gol, Norway, May 8-11, 1989.

Point of contact: R. C. Wingrove, Ames Research Center, MS 210-9, Moffett Field, CA 94035
(415) 694-5429 or FTS 464-5429

16. Abstract

Advanced methods have been developed to determine time-varying winds and turbulence from digital flight-data recorders carried aboard modern airliners. Analysis of several cases involving severe clear-air turbulence encounters at cruise altitudes has shown that the aircraft encountered vortex arrays generated by destabilized wind-shear layers above mountains or thunderstorms. A model has been developed to identify the strength, size, and spacing of vortex arrays. This model is used to study the effects of severe wind hazards on operational safety for different types of aircraft. The study demonstrates that small remotely piloted vehicles and executive aircraft exhibit more violent behavior than do large airliners during encounters with high-altitude vortices. Analysis of digital flight data from the accident at Dallas/Ft. Worth in 1985 indicates that the aircraft encountered a microburst with rapidly changing winds embedded in a strong outflow near the ground. A multiple-vortex-ring model has been developed to represent the microburst wind pattern. This model can be used in flight simulators to better understand the control problems in severe microburst encounters.

17. Key Words (Suggested by Author(s)) Aircraft dynamics Clear air turbulence Microbursts Vortex models	18. Distribution Statement Unclassified — Unlimited Subject category — 03

19. Security Classif. (of this report) Unclassified	20. Security Classif. (of this page) Unclassified	21. No. of pages 9	22. Price A02

NASA FORM 1626 OCT 86